Macromolecules **1986,** *19,* 2779–2787

Estimation of Monomer Reactivity Ratios by the Error-in-Variable Method

K. K. Chee* and S. C. Ng

Department of Chemistry, University of Malaya, Kuala Lumpur, Malaysia.
Received May 30, 1984

ABSTRACT: The integrated copolymerization equation is converted to a form that is more accessible. Applying the refined least-squares adjustment procedure to this particular expression allows the monomer reactivity ratios to be estimated with great accuracy. The simulated copolymerization data on a total of ten representative monomer pairs are investigated in this work. The results obtained by this novel approach are compared with those acquired by the linear and nonlinear least-squares analyses based on the differential and integrated copolymerization equations, respectively, at two distinct conversion levels and three different error structures. Apparently, the classical Fineman–Ross equation and the nonlinear least-squares calculations are far from adequate even at low conversion. Moreover, their predictions are rather arbitrary in that they are sensitive to inversion of experimental data. The precision of the estimates of monomer reactivity ratios is described by the 95% joint confidence limits.

Introduction

According to the familiar terminal model, the reaction kinetics of binary chain growth copolymerization are characterized by four principal propagation steps involving two distinct active chain ends. However, the overall results of the reaction may be well described by two monomer reactivity ratios, which are the relative rate constants for the additions of the chain ends to their own monomers and to the other monomers. These kinetic parameters usually refer to monomers 1 and 2 and are denoted by r_1 and r_2, respectively. They are obtainable experimentally by either sequence distribution or copolymer composition measurements.[1] Although the former practice is more efficient, it requires specific technique and instrumentation and is less popular than the latter approach, which is relevant to the present context.

A number of algorithms for estimating the monomer reactivity ratios have been reported and reviewed recently.[1-8] Among them are the linear least-squares (LLS) and nonlinear least-squares (NLS) analyses, as well as the error-in-variable method (EVM). All are associated with the copolymerization equations derived in 1944 by Alfrey et al.[9,10] In the present paper, the three distinct methods are compared critically in order to select the best one for r_1 and r_2 determinations. Also, various hypothetical copolymerizations are designed to assess the versatility of this novel procedure.

Estimation of Monomer Reactivity Ratios

The differential copolymerization equation depicts the copolymer composition in terms of the instantaneous mole fractions of monomers 1 and 2 in the copolymer, designated as F_1 and F_2, respectively, as a function of their respective instantaneous monomer concentrations $[M_1]$ and $[M_2]$:

$$\frac{F_1}{F_2} = \frac{[M_1]\{r_1[M_1] + [M_2]\}}{[M_2]\{[M_1] + r_2[M_2]\}} \tag{1}$$

Traditionally, eq 1 is applied to low conversion of monomers by replacing the concentrations $[M_1]$ and $[M_2]$ with the initial monomer feeds $[M_1]_0$ and $[M_2]_0$, respectively. Since the relative rate of adding the two monomers to the copolymer, $d[M_1]/d[M_2]$, is equal to the left-hand side of eq 1, eq 1 can be readily integrated to a closed form[10]

$$\ln x_2 = r_2 \ln x_1 + \frac{1 - r_1r_2}{1 - r_1} \ln\left[\frac{(1 - r_2)x_2 - (1 - r_1)x_2x}{(1 - r_2)x_2 - (1 - r_1)x_1x}\right] \tag{2}$$

where

$$x_1 = [M_1]/[M_1]_0 \tag{2a}$$

$$x_2 = [M_2]/[M_2]_0 \tag{2b}$$

$$x = [M_1]_0/[M_2]_0 \tag{2c}$$

The limitations and an alternative form of the equation are discussed in Appendix I.

It has been demonstrated that eq 1 can be transformed to several linear forms.[5] The well-known Fineman–Ross (FR) equation[13] is given as

$$G = r_1F - r_2 \tag{3}$$

where

$$F = x^2/y \tag{3a}$$

$$G = x(y - 1)/y \tag{3b}$$

$$y = F_1/F_2 \tag{3c}$$

However, by no means is eq 3 in an exact form, for the percent conversion of monomers to copolymer, which conspicuously affects the variable y, has been totally ignored herein. In the present investigation, this inherent defect is addressed by rearranging eq 2 to the form[4]

$$r_2 = Q \tag{4}$$

where

$$Q = \frac{\ln x_2 - \ln X/p}{\ln x_1 + \ln X} \tag{4a}$$

with

$$X = \frac{x_2(1 - xp)}{x_2 - xx_1p} \tag{4b}$$

$$p = (1 - r_1)/(1 - r_2) \tag{4c}$$

Indeed, it has been shown that the results obtained by the least-squares treatments of eq 1 and its transformed versions are biased due to the complete disregard of the error structure of the observations.[14,15] In view of this, we resort to the EVM method,[4,16,17] which takes into account this important factor. Other important features of this rigorous approach have been discussed elsewhere.[18,19]

Basically, the EVM method minimizes the sum of the weighted squares of the residual of r_2,[20] defined by

0024-9297/86/2219-2779$01.50/0

$$S = \sum_x W f^2 \tag{5}$$

where

$$f = r_2 - Q \tag{5a}$$

Hereafter, the summation refers to a set of n experimental data x and y. The weight W is related to the variance of f as outlined in Appendix II. With the knowledge of the first approximations p' and r_2' obtained by a unique method elaborated in Appendix III, the function f can be expressed by a Taylor series truncated after the first power terms of p and r_2. Equation 5 is then differentiated with respect to p and r_2 to produce two normal equations that result in the second approximations of p and r_2, given respectively as

$$p'' = \frac{\sum AB \sum BC - \sum B^2 \sum AC}{\sum A^2 \sum B^2 - (\sum AB)^2} \tag{6}$$

$$r_2'' = \frac{\sum AB \sum AC - \sum A^2 \sum BC}{\sum A^2 \sum B^2 - (\sum AB)^2} \tag{7}$$

where

$$A = W'^{1/2}\left(\frac{\partial f}{\partial p}\right)_{p',r_2'} + \frac{1}{2}\frac{1}{W'^{1/2}}\left(\frac{\partial W}{\partial p}\right)_{p',r_2'} \tag{7a}$$

$$B = W'^{1/2}\left(\frac{\partial f}{\partial r_2}\right)_{p',r_2'} \tag{7b}$$

$$C = W'^{1/2}\left\{f(p',r_2') - p'\left[\left(\frac{\partial f}{\partial p}\right)_{p',r_2'} + \frac{1}{2W'}\left(\frac{\partial W}{\partial p}\right)_{p',r_2'}\right] - r_2'\left(\frac{\partial f}{\partial r_2}\right)_{p',r_2'}\right\} \tag{7c}$$

and the weight W' is based on p' and r_2'. Finally, the final values of p and r_2, designated respectively as $\hat{p}$ and $\hat{r}_2$, are obtained by an iterative method involving eq 6 and 7. The variances of $\hat{p}$ and $\hat{r}_2$ are respectively

$$\mathrm{Var}\ (\hat{p}) = \frac{\sum B_0^2}{\sum A_0^2 \sum B_0^2 - (\sum A_0 B_0)^2} \tag{8}$$

$$\mathrm{Var}\ (\hat{r}_2) = \frac{\sum A_0^2}{\sum A_0^2 \sum B_0^2 - (\sum A_0 B_0)^2} \tag{9}$$

and the covariance of $\hat{p}$ and $\hat{r}_2$ is

$$\mathrm{Cov}\ (\hat{p},\hat{r}_2) = \frac{\sum A_0 B_0}{\sum A_0^2 \sum B_0^2 - (\sum A_0 B_0)^2} \tag{10}$$

where A_0 and B_0 are respectively the values of A and B computed at $p' = p^0$ and $r_2' = r_2^0$ using eq 7a and 7b. Here the point (p^0,r_2^0) refers to the pair of p and r_2 that would lead to the estimates $\hat{p}$ and $\hat{r}_2$ by the last iterative step. The estimate of r_1 and its variance are written respectively as

$$\hat{r}_1 = 1 - (1 - \hat{r}_2)\hat{p} \tag{11}$$

$$\mathrm{Var}\ (\hat{r}_1) = \hat{p}^2\ \mathrm{Var}\ (\hat{r}_2) + (1 - \hat{r}_2)^2\ \mathrm{Var}\ (\hat{p}) - 2(1 - \hat{r}_2)\hat{p}\ \mathrm{Cov}\ (\hat{p},r_2) \tag{12}$$

It is noted that the foregoing calculations can be readily adapted to produce the NLS results by merely setting $W = 1$ and $(\partial W/\partial p)_{p',r_2'} = 0$ in eq 5–7. However, the variances and covariances are now computed by the following approximate equations:

$$\mathrm{Var}\ (\hat{p}) = \mathrm{Var}\ (f)\left[\frac{B_0 \sum A_0 B_0 - A_0 \sum B_0^2}{\sum A_0^2 \sum B_0^2 - (\sum A_0 B_0)^2}\right]^2 \tag{13}$$

$$\mathrm{Var}\ (\hat{r}_2) = \mathrm{Var}\ (f)\left[\frac{A_0 \sum A_0 B_0 - B_0 \sum A_0^2}{\sum A_0^2 \sum B_0^2 - (\sum A_0 B_0)^2}\right]^2 \tag{14}$$

$$\mathrm{Cov}\ (\hat{p},\hat{r}_2) = \mathrm{Var}\ (f)\left[\frac{(B_0 \sum A_0 B_0 - A_0 \sum B_0^2)(A_0 \sum A_0 B_0 - B_0 \sum A_0^2)}{[\sum A_0^2 \sum B_0^2 - (\sum A_0 B_0)^2]^2}\right] \tag{15}$$

where

$$\mathrm{Var}\ (f) = \frac{\sum (A_0 \hat{p} + B_0 \hat{r}_2 + C_0)^2}{n - 2} \tag{15a}$$

The same NLS technique has been applied to the differential copolymerization equation by other workers.[14,15]

According to the principle of maximum likelihood applying to eq 5, the residues of r_2 $(=W^{1/2}f)$ arising from the random errors of measurements are assumed to conform to the same Gaussian distribution as observed by the EVM model.[20] However, this assumption is invalid for the NLS analysis, since Var (f) is not a constant. In the present investigation, the implications of the substantial difference between the two distinct algorithms are highlighted by their results acquired under various simulated copolymerization conditions.

Results and Discussion

The copolymer composition data for 60 hypothetical systems were derived by computer simulation. The true values of the monomer reactivity ratios, r_1^* and r_2^*, for these systems are displayed in Table I. The true copolymer composition F_1^* for a particular monomer pair characterized by r_1^* and r_2^* was computed by using eq A-1, A-4, and A-5 at a fixed true degree of conversion P_n^* and a given true initial monomer feed f_{10}^*. The value of $\bar{\alpha}$ is 1.5, unless otherwise specified. In this connection, the values of f_{10}^* chosen cover the practical range 0.1–0.9. Altogether, eight or nine sets of these data were generated for each of these systems. To make the simulation more realistic, the values of F_1^*, f_{10}^*, and P_n^* were compounded with three different sets of errors. These are the normally distributed random errors with mean zero and standard deviations (i.e., square roots of variances) $\epsilon_P = \epsilon_f = 0.004$, whereas $\epsilon_F = 0.005$, 0.012, or 0.020 for each of these monomer pairs.

On the basis of the above data, a series of calculations was performed as follows. First, the procedure described in Appendix III was employed to search for the first approximations p' and r_2'. These values were then utilized to compute the final values $\hat{p}$ and $\hat{r}_2$ following the iterative algorithm introduced in the preceding section. Meanwhile the FR equation was treated by the LLS method in the usual manner. All the mathematical computations were carried out by a Univac 1100/60 computer system.[2] The results on $\hat{r}_1$ and $\hat{r}_2$ at the two levels of conversion $P_n^* = 0.05$ and 0.50 for the 60 systems divided according to the values of ϵ_F are displayed in Table I, which also lists their respective standard deviations from the two iterative methods. The monomer pair number 9 may be converted to number 10 by interchanging the monomers and vice versa.

Figure 1 is the FR plot with G vs. F for system 1A. The linearity of this relationship is substantiated by its linear correlation coefficient, whose value, included in Table IA,

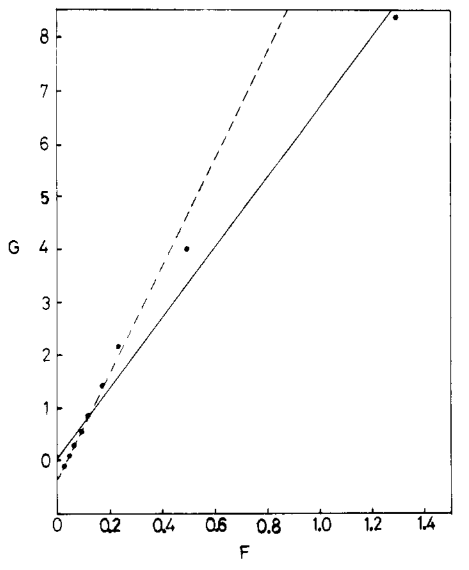

Figure 1. Fineman–Ross plot for system 1A. The solid line is the linear least-squares fit of the "experimental" data points designated by filled circles. The dashed line is based on the true values r_1* and r_2*.

is close unity. However, the straight line registers the most unsatisfactory results since a negative value, indicating a physically infeasible state, is reported for r_2! The theoretical line is drawn to illustrate implicitly that the errors in G at various F values for this particular system actually do not comply to the same distribution as demanded by the normal linear least-squares practice. This deficiency of the model is also observed in other FR plots.

To facilitate the ensuing discussion, a useful parameter is defined as

$$\Delta R = 100\left\{\sum_i \left[\left(\frac{\hat{r}_1 - \hat{r}_1^*}{r_1^*}\right)_i^2 + \left(\frac{\hat{r}_2 - \hat{r}_2^*}{r_2^*}\right)_i^2\right]^{1/2}\right\} \Big/ m \qquad (16)$$

where the subscript i refers to the ith system and m is the total number of systems with the same degree of conversion and error design. This index is employed to indicate the average accuracy of a particular estimation scheme. For example, a small $\overline{\Delta R}$ value, reflecting that, in general, the $\hat{r}_1$ and $\hat{r}_2$ estimates are relatively close to their respective true values r_1* and r_2*, may imply an accurate and reliable method. The values of $\overline{\Delta R}$ computed from Table I are exhibited in Table II. Comparatively, Table II shows that the FR predictions are usually unacceptable even at low conversion. Nevertheless, this adverse situation can be improved with the NLS approach, whose $\overline{\Delta R}$ values are consistently lower than those of the FR method. This means that the conversion factor P_n may play a vital role in this connection.

As expected, both the FR and NLS estimates of r_1 and r_2 are highly biased under the present error structures, which are similar to those observed experimentally.[3,8] These unfavorable outcomes may be attributed to the irregular distributions of the errors in various observed parameters as witnessed in Figure 1. Herein, the EVM method is applied to overcome this shortcoming. Table II demonstrates that the weighted least-squares analysis is indeed more accurate than the ordinary least-squares calculations by generally at least 3-fold in terms of the $\overline{\Delta R}$ index. However, the magnitude of these differences reduces noticeably when the errors of measurements increase significantly. Besides, Table II suggests that, in any case, it is advantageous to use the low-conversion data for the estimations of monomer reactivity ratios as they usually lead to more satisfactory results. The pronounced effects of the error structure on the present analyses are apparent. Referring to the EVM results in Table II, we note that empirically the $\overline{\Delta R}$ index increases linearly with ϵ_F at constant P_n*. More strikingly, the NLS interactions actually fail to converge to the final $\hat{p}$ and $\hat{r}_2$ at moderate and high ϵ_F for a number of systems (Table IB,C).

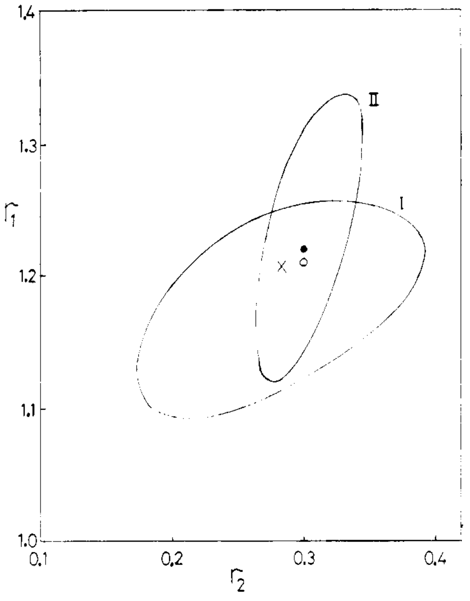

Figure 2. 95% joint confidence limits for system 4A: (●) true values; (○) EVM estimates; (×) NLS estimates. Ellipses I and II are respectively obtained by the NLS and EVM methods.

In some cases, the negative values of $\hat{r}_1$ and $\hat{r}_2$ are reported by the two simple least-squares procedures in Table I. On the other hand, there are instances where the linear least-squares treatment seems to outperform the EVM method as in systems 6F, 9C, and 9E. However, the former is exceptionally sensitive to an effect of reindexing the monomers as inferred from the results on monomer pairs 9 and 10 in Table I. Analogously, the NLS procedure is equally susceptible to such a data transformation which does not change the EVM predictions appreciably. In this sense, the FR and NLS models may actually produce fictitious values of $\hat{r}_1$ and $\hat{r}_2$. Certainly, the EVM procedure is the best choice in deriving the most accurate and dependable parameter estimaters in any event. This observation is parallel to that reported by Sutton and MacGregor,[22] who have analyzed vapor–liquid equilibrium data by various algorithms, including the EVM technique.

From a statistical point of view, the uncertainty of the estimates is best represented by the joint confidence contour[23] rather than their individual confidence intervals or standard deviations. Figure 2 exhibits a typical plot of the elliptical 95% joint confidence limits constructed by the procedure outlined in Appendix IV for system 4A. Since the area of ellipse I is indisputably larger than that of ellipse II, it implies that the EVM method is more reliable than its simplified counterpart.[3,15] However, the comparison is rather obscure if the standard deviation data in Table IA are inferred for the same system. Plots analogous to Figure 2 for other copolymerizations are not presented herein. Figure 3A confirms that the precision of EVM estimates decreases with increasing P_n* (systems 6C and 6D) and ϵ_F (systems 6A, 6C, and 6E) for r_1* = 0.50 and r_2* = 0.40. Recently, O'Driscoll et al. studied the high-conversion free radical copolymerization of styrene

Table I

A. Estimates of $\hat{r}_1$ and $\hat{r}_2$ Obtained by Various Methods Based on $\epsilon_f = \epsilon_P = 0.004$ and $\epsilon_F = 0.005$

system		method					
		A $P_n^* = 0.05$ ($\bar{\alpha} = 1.5$)			B $P_n^* = 0.50$ ($\bar{\alpha} = 1.5$)		
		FR	NLS	EVM	FR	NLS	EVM
1	$r_1^* = 10.00$	6.606	9.401 (2.248)[b]	10.010 (1.127)[b]	5.668	8.853 (1.158)	10.170 (1.550)
	$r_2^* = 0.30$	−0.073 (0.9926)[a]	0.298 (0.098)[c]	0.306 (0.026)[c]	0.573 (0.9939)	0.266 (0.049)	0.306 (0.036)
2	$r_1^* = 10.00$	6.556	8.884 (1.592)	9.901 (0.597)	5.678	8.668 (0.906)	10.369 (1.024)
	$r_2^* = 0.10$	−0.234 (0.9927)	0.063 (0.088)	0.101 (0.012)	0.347 (0.9921)	0.074 (0.044)	0.107 (0.022)
3	$r_1^* = 2.00$	1.829	1.917 (0.060)	1.990 (0.057)	1.616	1.911 (0.058)	2.068 (0.086)
	$r_2^* = 0.10$	0.054 (0.9994)	0.079 (0.027)	0.102 (0.006)	0.250 (0.9991)	0.086 (0.023)	0.107 (0.011)
4	$r_1^* = 1.22$	1.169	1.208 (0.021)	1.211 (0.037)	1.117	1.207 (0.026)	1.274 (0.052)
	$r_2^* = 0.30$	0.285 (0.9995)	0.283 (0.029)	0.304 (0.012)	0.436 (0.9993)	0.285 (0.033)	0.306 (0.017)
5	$r_1^* = 0.90$	0.909	0.911 (0.008)	0.910 (0.021)	0.912	0.911 (0.010)	0.910 (0.029)
	$r_2^* = 0.10$	0.113 (0.9998)	0.103 (0.013)	0.098 (0.005)	0.236 (0.9997)	0.104 (0.016)	0.098 (0.008)
6	$r_1^* = 0.50$	0.507	0.512 (0.026)	0.517 (0.017)	0.623	0.511 (0.033)	0.516 (0.023)
	$r_2^* = 0.40$	0.412 (0.9993)	0.390 (0.020)	0.0399 (0.012)	0.554 (0.9989)	0.388 (0.024)	0.397 (0.017)
7	$r_1^* = 0.45$	0.461	0.407 (0.037)	0.451 (0.119)	0.583	0.500 (0.119)	0.450 (0.198)
	$r_2^* = 0.82$	0.828 (0.9991)	0.807 (0.010)	0.823 (0.020)	0.874 (0.9985)	0.848 (0.032)	0.835 (0.032)
8	$r_1^* = 0.10$	0.106	0.099 (0.012)	0.098 (0.009)	0.215	0.101 (0.016)	0.097 (0.014)
	$r_2^* =0.10$	0.110 (0.998)	0.105 (0.006)	0.098 (0.004)	0.245 (0.9889)	0.108 (0.008)	0.098 (0.007)
9	$r_1^* = 0.03$	0.033	0.039 (0.015)	0.029 (0.023)	0.080	0.078 (0.015)	0.026 (0.030)
	$r_2^* = 0.30$	0.305 (0.9987)	0.312 (0.007)	0.299 (0.009)	0.375 (0.9410)	0.293 (0.007)	0.293 (0.012)
10[d]	$r_1^* = 0.30$	0.309	0.306 (0.015)	0.329 (0.008)	0.460	0.286 (0.017)	0.327 (0.011)
	$r_2^* = 0.03$	0.042 (0.9994)	0.023 (0.011)	0.029 (0.003)	0.237 (0.9989)	0.043 (0.011)	0.026 (0.006)

B. Estimates of $\hat{r}_1$ and $\hat{r}_2$ Obtained by Various Methods Based on $\epsilon_f = \epsilon_P = 0.004$ and $\epsilon_F = 0.012$

system		method					
		C $P_n^* = 0.05$ ($\bar{\alpha} = 1.5$)			D $P_n^* = 0.50$ ($\bar{\alpha} = 1.5$)		
		FR	NLS	EVM	FR	NLS	EVM
1	$r_1^* = 10.00$	4.264	*e*	9.043 (1.520)[b]	3.879	8.580 (2.771)[b]	9.646 (2.469)
	$r_2^* = 0.30$	−0.402 (0.9769)[a]	*e*	0.268 (0.036)[c]	0.130 (0.9798)	0.277 (0.113)[c]	0.290 (0.059)
2	$r_1^* = 10.00$	4.233	*e*	9.150 (0.930)	3.797	7.152 (1.899)	10.160 (1.853)
	$r_2^* = 0.10$	−0.519 (0.9775)	*e*	0.086 (0.016)	−0.151 (0.9787)	0.015 (0.115)	0.110 (0.039)
3	$r_1^* = 2.00$	1.564	1.759 (0.132)	1.985 (0.113)	1.389	1.677 (0.120)	2.060 (0.175)
	$r_2^* = 0.10$	−0.066 (0.9972)	0.045 (0.068)	0.098 (0.011)	0.079 (0.9974)	0.027 (0.066)	0.109 (0.021)
4	$r_1^* = 1.22$	1.043	*e*	1.211 (0.072)	1.001	1.002 (0.027)	1.275 (0.101)
	$r_2^* = 0.30$	0.193 (0.9984)	*e*	0.298 (0.021)	0.341 (0.9982)	0.193 (0.066)	0.300 (0.032)
5	$r_1^* = 0.90$	0.965	1.002 (0.022)	0.913 (0.045)	0.981	1.002 (0.024)	0.912 (0.059)
	$r_2^* = 0.10$	0.141 (0.9984)	0.136 (0.032)	0.099 (0.010)	0.298 (0.9981)	0.132 (0.033)	0.094 (0.016)
6	$r_1^* = 0.50$	0.469	0.528 (0.052)	0.511 (0.034)	0.575	0.530 (0.066)	0.504 (0.045)
	$r_2^* = 0.40$	0.361 (0.9988)	0.384 (0.041)	0.386 (0.024)	0.491 (0.9987)	0.376 (0.053)	0.375 (0.034)

Table I (Continued)

B. Estimates of $\hat{r}_1$ and $\hat{r}_2$ Obtained by Various Methods Based on $\epsilon_f = \epsilon_P = 0.004$ and $\epsilon_F = 0.012$

		method					
		C			D		
		$P_n^* = 0.05$ ($\bar{\alpha} = 1.5$)			$P_n^* = 0.50$ ($\bar{\alpha} = 1.5$)		
system		FR	NLS	EVM	FR	NLS	EVM
7	$r_1^* = 0.45$	0.428	0.318	0.439	0.616	*e*	0.463
			(0.097)	(0.197)			(0.205)
	$r_2^* = 0.82$	0.770	0.777	0.818	0.914	*e*	0.876
		(0.9984)	(0.028)	(0.034)	(0.9971)	*e*	(0.026)
8	$r_1^* = 0.10$	0.113	0.105	0.105	0.356	0.109	0.097
			(0.029)	(0.019)		(0.031)	(0.029)
	$r_2^* = 0.10$	0.127	0.114	0.099	0.520	0.116	0.091
		(0.9988)	(0.014)	(0.009)	(0.9858)	(0.015)	(0.014)
9	$r_1^* = 0.03$	0.030	−0.021	0.026	0.070	0.073	0.018
			(0.036)	(0.047)		(0.042)	(0.061)
	$r_2^* = 0.30$	0.297	0.332	0.289	0.369	0.287	0.279
		(0.9924)	(0.018)	(0.017)	(0.8419)	(0.021)	(0.024)
10[d]	$r_1^* = 0.30$	0.288	0.351	0.327	0.490	0.282	0.224
			(0.036)	(0.018)		(0.045)	(0.023)
	$r_2^* = 0.03$	0.011	0.004	0.027	0.290	0.070	0.018
		(0.9990)	(0.027)	(0.006)	(0.9979)	(0.030)	(0.014)

C. Estimates of $\hat{r}_1$ and $\hat{r}_2$ Obtained by Various Methods Based on $\epsilon_f = \epsilon_P = 0.004$ and $\epsilon_F = 0.020$

		method					
		E			F		
		$P_n^* = 0.05$ ($\bar{\alpha} = 1.5$)			$P_n^* = 0.50$ ($\bar{\alpha} = 1.5$)		
system		FR	NLS	EVM	FR	NLS	EVM
1	$r_1^* = 10.00$	2.977	*e*	7.721	2.796	*e*	8.444
				(1.594)[b]			(2.720)
	$r_2^* = 0.30$	−0.590	*e*	0.220	−0.148	*e*	0.249
		(0.9640)[a]		(0.042)[c]	(0.9663)		(0.076)
2	$r_1^* = 10.00$	2.957	*e*	8.030	2.650	*e*	9.136
				(1.109)			(2.313)
	$r_2^* = 0.10$	−0.682	*e*	0.066	−0.577	*e*	0.098
		(0.9650)		(0.020)	(0.9707)		(0.056)
3	$r_1^* = 2.00$	1.328	1.669	1.903	1.192	1.418	2.061
			(0.241)[b]	(0.172)		(0.144)	(0.270)
	$r_2^* = 0.10$	−0.175	0.046	0.092	−0.049	−0.038	0.107
		(0.9929)	(0.121)[c]	(0.016)	(0.9937)	(0.111)	(0.035)
4	$r_1^* = 1.22$	0.922	*e*	1.212	0.888	*e*	1.215
				(0.108)			(0.151)
	$r_2^* = 0.30$	0.104	*e*	0.289	0.247	*e*	0.286
		(0.9958)		(0.032)	(0.9955)		(0.050)
5	$r_1^* = 0.90$	1.032	1.081	0.913	1.049	1.083	0.911
			(0.044)	(0.075)		(0.053)	(0.096)
	$r_2^* = 0.10$	0.174	0.173	0.101	0.337	0.178	0.090
		(0.9950)	(0.057)	(0.016)	(0.9951)	(0.057)	(0.024)
6	$r_1^* = 0.50$	0.431	0.585	0.494	0.525[f]	*e*	0.474
			(0.083)	(0.052)			(0.069)
	$r_2^* = 0.40$	0.308	0.354	0.364	0.426	*e*	0.335
		(0.9975)	(0.072)	(0.037)	(0.9975)		(0.053)
7	$r_1^* = 0.45$	0.394	0.234	0.440	0.654	*e*	0.452
			(0.157)	(0.120)			(0.388)
	$r_2^* = 0.82$	0.709	0.749	0.871	0.963	*e*	0.884
		(0.9966)	(0.044)	(0.016)	(0.9914)		(0.045)
8	$r_1^* = 0.10$	0.121	0.059	0.107	0.379	0.076	0.089
			(0.049)	(0.031)		(0.055)	(0.044)
	$r_2^* = 0.10$	0.147	0.126	0.099	0.566	0.140	0.083
		(0.9968)	(0.024)	(0.015)	(0.9833)	(0.026)	(0.022)
9	$r_1^* = 0.03$	0.027	−0.006	0.023	0.058	0.080	0.008
			(0.066)	(0.071)		(0.079)	(0.094)
	$r_2^* = 0.30$	0.290	0.349	0.278	0.364	0.286	0.259
		(0.9762)	(0.031)	(0.027)	(0.6790)	(0.039)	(0.038)
10[d]	$r_1^* = 0.30$	0.266	*e*	0.324	0.528	0.287	0.216
				(0.027)		(0.080)	(0.037)
	$r_2^* = 0.03$	−0.022	*e*	0.023	0.355	0.105	0.008
		(0.9980)		(0.009)	(0.9959)	(0.052)	(0.021)

[a] Linear correlation coefficient. [b] Standard deviation of $\hat{r}_1$. [c] Standard deviation of $\hat{r}_2$. [d] The value of $\bar{\alpha}$ is 0.6667. [e] No results are obtained. [f] Reindexing the monomers results in the following: FR, $\hat{r}_1 = 0.586$, $\hat{r}_2 = 0.510$ (0.9982);[a] NLS, $\hat{r}_1 = 0.570$ (0.060),[b] $\hat{r}_2 = 0.326$ (0.119);[c] EVM, $\hat{r}_1 = 0.464$ (0.058),[b] $\hat{r}_2 = 0.333$ (0.121).[c]

and methyl methacrylate by means of UV and NMR spectroscopy.[8] They revealed that the confidence regions for r_1 and r_2 after the EVM analysis depend dramatically upon the experimental techniques applied for copolymer analysis. Incidentally, these contour maps resemble Figure 3A. For system 6C in Figure 3B, the 95% joint confidence

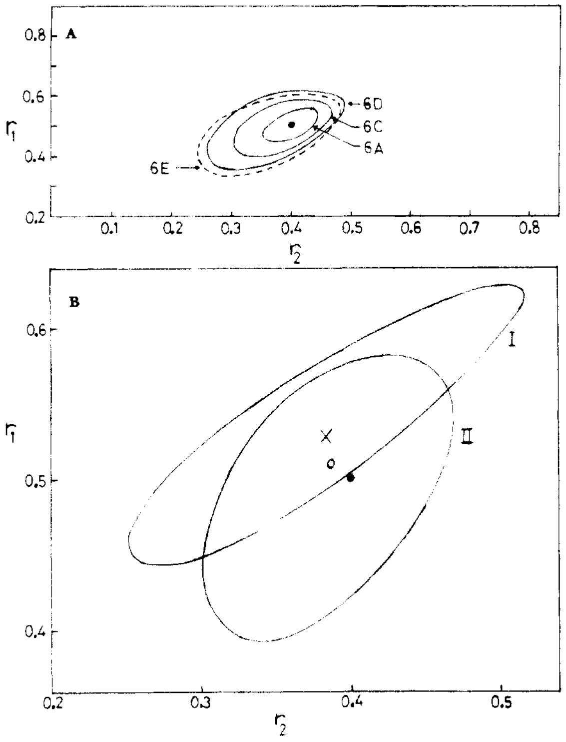

Figure 3. Comparison of 95% joint confidence limits: (A) obtained by the EVM method for systems 6A, 6C, 6D, and 6E; (B) obtained by the NLS and EVM methods for system 6C. Designations are as in Figure 2.

limits of the NLS scheme are slightly smaller than those of its refined version, but the theoretical datum (r_1^*,r_2^*), which falls near the center of elliptical contour II, virtually lies outside elliptical contour I. Hence, the NLS method is marginally more precise and yet much less accurate than the EVM method in this particular case. This peculiar situation is also applicable to a few other systems envisaged. However, the reliability of the statistically sound procedure is basically not affected.

We have thus put forward an elegant procedure that meets all five criteria recommended by Tidwell and Mortimer[6] for determining monomer reactivity ratios. Perhaps one of the unique features of this EVM method is that it demands maximum input information, including a knowledge of the various experimental uncertainties, and hence would give rise to efficient estimates. Practically, the error structures may be evaluated by replicating the experiments.[23] In the present analyses, the integrated copolymerization equation is recast to the form of eq 4, which can generate the p' and r_2' data by itself without resorting to other equations as commonly practiced elsewhere.[14,16] These initial approximations of monomer reactivity ratios are indeed satisfactory in that no more than 21 successive operations are required to finalize the results listed in Table I by the iterative process. Another main feature of this study is the utility of an exact expression for the variance of f into which the covariance terms are incorporated.

In summary, the EVM method is superior to the LLS and NLS analyses in estimating the monomer reactivity ratios. The predictions of this refined model based on an integrated copolymerization equation compare remarkably well with the theory for a wide range of monomer pairs with r_1^*/r_2^* varying from 0.1 to 100. More importantly, unlike the two statistically inferior ones, the EVM procedure is relatively more symmetrical to the method of designating the monomers. However, it is less effective with respect to larger experimental errors, particularly for monomer pairs whose monomer reactivity ratios are greatly different even at low conversion. Generally, increasing the degree of conversion would lead to less accurate results. The joint confidence contours are more informative than the standard deviations in describing the precision of $\hat{r}_1$ and $\hat{r}_2$ in the present context. In any case, these findings are not susceptible to the factor $\bar{\alpha}$, which has a value around 1.0 usually.

Appendix I

Skeist[11] and Meyer et al.[12] have established an equivalent form of eq 2; viz.

$$P_n = 1 - \left(\frac{f_1}{f_{10}}\right)^{\alpha}\left(\frac{f_2}{f_{20}}\right)^{\beta}\left(\frac{f_{10}-\delta}{f_1-\delta}\right)^{\gamma} \qquad \text{(A-1)}$$

where

$$\alpha = r_2/(1 - r_2) \qquad \text{(A-1a)}$$

$$\beta = r_1/(1 - r_1) \qquad \text{(A-1b)}$$

$$\gamma = (1 - r_1r_2)/[(1 - r_1)(1 - r_2)] \qquad \text{(A-1c)}$$

$$\delta = (1 - r_2)/(2 - r_1 - r_2) \qquad \text{(A-1d)}$$

$$f_1 = 1 - f_2 = [\mathrm{M}_1]/([\mathrm{M}_1] + [\mathrm{M}_2]) \qquad \text{(A-1e)}$$

$$f_{10} = 1 - f_{20} = [\mathrm{M}_1]_0/([\mathrm{M}_1]_0 + [\mathrm{M}_2]_0) \qquad \text{(A-1f)}$$

It is noted that both eq 2 and A-1 are subject to the following restrictions:

(1) $r_1 \neq 1$ and $r_2 \neq 1$

(2) If $r_1 = 1$, then

$$r_2 = \frac{x_2 \ln x_2 - x_1}{x_2 \ln x_1} \qquad \text{(A-2)}$$

(3) If $r_2 = 1$, then

$$r_1 = \frac{1}{\ln x_2}\left[\ln x_1 + \frac{x_1 - x_2}{xx_1}\right] \qquad \text{(A-3)}$$

(4) For azeotropic copolymerization in which $x_1 = x_2 = 1$ (eq 2) or $f_1 = f_{10} = \delta$ (eq A-1), the equations are trivial. Here, we have

$$x_1 = \frac{f_1}{f_{10}}(1 - P_n) = 1 - \frac{F_1P_n}{f_{10}} \qquad \text{(A-4)}$$

$$x_2 = \frac{f_2}{f_{20}}(1 - P_n) = 1 - \frac{F_2P_n}{f_{20}} \qquad \text{(A-5)}$$

$$x = f_{10}/f_{20} \qquad \text{(A-6)}$$

where the experimental variables

$$F_1 = 1 - F_2 = \frac{[\mathrm{M}_1]_0 - [\mathrm{M}_1]}{([\mathrm{M}_1]_0 + [\mathrm{M}_2]_0) - ([\mathrm{M}_1] + [\mathrm{M}_2])} \qquad \text{(A-7)}$$

$$P_n = \frac{([\mathrm{M}_1]_0 + [\mathrm{M}_2]_0) - ([\mathrm{M}_1] + [\mathrm{M}_2])}{[\mathrm{M}_1]_0 + [\mathrm{M}_2]_0} \qquad \text{(A-8)}$$

The degree of conversion, P_n, is related to the weight percent conversion, $100P_w$, by

$$P_n = P_w\frac{(1 + y)(1 + \bar{\alpha}x)}{(1 + x)(1 + \bar{\alpha}y)} \qquad \text{(A-9)}$$

where

$$\bar{\alpha} = M_1/M_2 \qquad \text{(A-9a)}$$

where M_1 and M_2 are respectively equal to the molecular

Table II
Comparison of $\overline{\Delta R}$ Values Calculated from Table I for Various $P_n{}^*$-ϵ_F Series

series			method		
no.	$P_n{}^*$	ϵ_F	FR	NLS	EVM
A	0.05	0.005	60	15	3
B	0.50	0.005	178	30	6
C	0.05	0.012	122	58	8
D	0.50	0.012	216	62	15
E	0.05	0.020	179	55	16
F	0.50	0.020	298	137	25

weights of monomers 1 and 2.

Appendix II

According to the rule of error propagation, the variance of function f at r_1 and r_2 is given as

$$\mathrm{Var}\ (f) = \left(\frac{\partial f}{\partial x}\right)^2 \mathrm{Var}\ (x) + \left(\frac{\partial f}{\partial y}\right)^2 \mathrm{Var}\ (y) + \left(\frac{\partial f}{\partial P_n}\right)^2 \mathrm{Var}\ (P_n) + 2\left(\frac{\partial f}{\partial x}\right)\left(\frac{\partial f}{\partial y}\right) \mathrm{Cov}\ (x,y) + 2\left(\frac{\partial f}{\partial y}\right)\left(\frac{\partial f}{\partial P_n}\right) \mathrm{Cov}\ (y,P_n) + 2\left(\frac{\partial f}{\partial x}\right)\left(\frac{\partial f}{\partial P_n}\right) \mathrm{Cov}\ (x,P_n) \tag{A-10}$$

Practically, the response variables x and y are calculated by

$$x = f_{10}/(1 - f_{10}) \tag{A-11}$$

$$y = F_1/(1 - F_1) \tag{A-12}$$

Another measurable quantity is the weight percent conversion, $100P_\mathrm{w}$, which is related to P_n by eq A-9. If the standard deviations of f_{10}, F_1, and P_w are dnoted by ϵ_f, ϵ_F, and ϵ_P, respectively, then the variance relationships can be approximated as follows:

$$\mathrm{Var}\ (x) = (1 + x)^4\epsilon_f{}^2 \tag{A-13}$$

$$\mathrm{Var}\ (y) = (1 + y)^4\epsilon_F{}^2 \tag{A-14}$$

$$\mathrm{Var}\ (P_n) = P_n\left\{\left(\frac{\epsilon_P}{P_\mathrm{w}}\right)^2 + (1 - \bar{\alpha})^2\left[\left(\frac{x}{1 + \bar{\alpha}x}\right)^2\left(\frac{\epsilon_f}{f_{10}}\right)^2 + \left(\frac{y}{1 + \bar{\alpha}y}\right)\left(\frac{\epsilon_F}{F_1}\right)^2\right]\right\} \tag{A-15}$$

Assuming that x and y are mutually independent, the following covariances may be written:

$$\mathrm{Cov}\ (x,y) = 0 \tag{A-16}$$

$$\mathrm{Cov}\ (y,P_n) = \rho\epsilon_y\epsilon_{P'} = \left(\frac{\partial P_n}{\partial y}\right)\epsilon_y{}^2 \tag{A-17}$$

$$\mathrm{Cov}\ (x,P_n) = \rho'\epsilon_x\epsilon_{p'} = \left(\frac{\partial P_n}{\partial x}\right)\epsilon_x{}^2 \tag{A-18}$$

where ρ and ρ' are the relevant correlation coefficients and

$$\epsilon_x = (\mathrm{Var}\ (x))^{1/2} \tag{A-18a}$$

$$\epsilon_y = (\mathrm{Var}\ (y))^{1/2} \tag{A-18b}$$

$$\epsilon_{P'} = (\mathrm{Var}\ (P_n))^{1/2} \tag{A-18c}$$

Here the derivatives $\partial f/\partial x$, $\partial f/\partial y$, and $\partial f/\partial P_n$ are obtainable from eq 5a and the other equations associated with it, whereas $\partial P_n/\partial x$ and $\partial P_n/\partial y$ are the derivatives of eq A-9. In this connection it is convenient to express the variables x_1 and x_2 in terms of the experimental parameters x, y, and P_n (or P_w) as

$$x_1 = 1 - \frac{y}{x}\left(\frac{1 + x}{1 + y}\right)P_n \tag{A-19}$$

$$x_2 = 1 - \left(\frac{1 + x}{1 + y}\right)P_n \tag{A-20}$$

The magnitudes of these error functions will of course depend primarily upon the experimental techniques employed to study the copolymerizations. However, in any event the weight of function f is given by

$$W = 1/\mathrm{Var}\ (f) \tag{A-21}$$

Appendix III

For low degree of conversion, the FR method may be useful for procuring the first set of approximations p' and r_2'. However, the direct approach is more general and effective for this particular purpose. Hence it will be pursued throughout the present investigations.

It can be shown from eq 5 by setting $\partial S/\partial p = \partial S/\partial r_2 = 0$ that

$$r_2 = \sum WQ/\sum W \tag{A-22}$$

$$\phi = 0 \tag{A-23}$$

where

$$\phi = r_2{}^2\sum\left(\frac{\partial W}{\partial p}\right) + 2r_2\sum W\left(\frac{\partial f}{\partial p}\right) - \sum Q\left(\frac{\partial W}{\partial p}\right) + \sum Q^2\left(\frac{\partial W}{\partial p}\right) - 2\sum WQ\left(\frac{\partial f}{\partial p}\right) \tag{A-24}$$

Since the parameters W, Q, $\partial f/\partial p$, and $\partial W/\partial p$ are functions of p only, a preset value of p ($p \neq 0$) can be substituted into eq A-22 to evaluate r_2, which then renders the functional value of ϕ via eq A-24. Subsequently, the values of S and r_1 can be determined respectively by using eq 5 and 4c. This exercise is repeated for an appropriate range of p values. Thus, a collection of these values that meets the requirements (1) $\phi \geq 0$, (2) $r_2 \geq 1.1$ or ≤ 0.9, (3) $r_1 \neq 1$, (4) r_1 and $r_2 \geq 0$ is then established. Among them, the p value that yields the smallest sum S is eventually selected as the first approximation p'. The corresponding r_2' results from eq A-22. It is noted that the first condition imposed on ϕ is in accordance with eq A-23, and the second restriction is necessary because the function f is indepenent of r_1 and tends to vanish as r_2 approaches unity, thus making the analysis trivial.

Appendix IV

The joint $100(1 - \theta)\%$ confidence region for $\hat{p}$ and $\hat{r}_2$ is bounded by the values of p and r_2 that satisfy the equation

$$\sum[A_0p + B_0r_2 + C_0]^2 = D_0{}^2 + 2S_m{}^2F_\theta(2,n-2) \tag{A-25}$$

where n is the total number of data points, A_0, B_0, and C_0 are defined in the text, and

$$D_0 = A_0\hat{p} + B_0\hat{r}_2 + C_0 \tag{A-26}$$

$$S_m{}^2 = \sum D_0{}^2/(n - 2) \tag{A-27}$$

The quantity $F_\theta(2,n-2)$ is the critical value of F from the F distribution. Now with the differences

$$\Delta p = p - \hat{p} \tag{A-28}$$

$$\Delta r_2 = r_2 - \hat{r}_2 \tag{A-29}$$

it can be shown by solving eq A-25 that the two extremes of Δr_2 are

$$\Delta r_2 = [-M \pm (M^2 - 4N)^{1/2}]/2 \qquad \text{(A-30)}$$

where

$$M = 2\left[\frac{\sum A_0B_0\sum A_0D_0 - \sum A_0{}^2\sum B_0D_0}{(\sum A_0B_0)^2 - \sum A_0{}^2\sum B_0{}^2}\right] \qquad \text{(A-31)}$$

$$N = \frac{(\sum A_0D_0)^2 + 2S_m{}^2F_\theta(2,n-2)\sum A_0{}^2}{(\sum A_0B_0)^2 - \sum A_0{}^2\sum B_0{}^2} \qquad \text{(A-32)}$$

It follows that

$$\Delta p = [-Q \pm (Q^2 - 4R)^{1/2}]/2 \qquad \text{(A-33)}$$

where

$$Q = \frac{2[\sum A_0D_0 + (\Delta r_2{}')\sum A_0B_0]}{\sum A_0{}^2} \qquad \text{(A-34)}$$

$$R = \frac{(\Delta r_2{}')^2\sum B_0{}^2 + 2(\Delta r_2{}')\sum B_0D_0 - 2S_m{}^2F_\theta(2,n-2)}{\sum A_0{}^2} \qquad \text{(A-35)}$$

Here, $\Delta r_2{}'$ can take any one of the values confined by

$$[-M - (M^2 - 4N)^{1/2}]/2 \le \Delta r_2{}' \le [-M + (M^2 - 4N)^{1/2}]/2 \qquad \text{(A-36)}$$

The values of r_1 and r_2 are computed by

$$r_2 = \hat{r}_2 + \Delta r_2 \qquad \text{(A-37)}$$

$$r_1 = 1 - (1 - r_2)(\hat{p} + \Delta p) \qquad \text{(A-38)}$$

Hence the locus of the joint confidence limit envelope in (r_1, r_2) space at the $100(1 - \theta)\%$ level may be determined by eq A-33 to A-38.

Nomenclature

α	parameter associated with eq A-1
$\bar{\alpha}$	ratio of M_1 and M_2
β	parameter associated with eq A-1
γ	parameter associated with eq A-1
δ	parameter associated with eq A-1
ϵ_f	standard deviation of f_{10}
ϵ_F	standard deviation of F_1
ϵ_P	standard deviation of P_w
ϵ_x	standard deviation of x
ϵ_y	standard deviation of y
$\epsilon_{P'}$	standard deviation of P_n
ρ	correlation coefficient associated with Cov (y,P_n)
ρ'	correlation coefficient associated with Cov (x,P_n)
ϕ	function defined by eq A-24
f	residual of r_2 (eq 5a)
f_1	instantaneous mole fraction of monomer 1 in the feed
f_2	instantaneous mole fraction of monomer 2 in the feed
f_{10}	initial mole fraction of monomer 1 in the feed
$f_{10}{}^*$	true value of f_1
f_{20}	initial mole fraction of monomer 2 in the feed
m	number of systems with the same degree of conversion and error structure
n	total number of sets of experimental data
p	parameter related to r_1 and r_2 (eq 4c)
p', p'', p^0	approximations of p
$\hat{p}$	final value (estimate) of p
P_n	degree of conversion (eq A-8)
$P_n{}^*$	true value of P_n
P_w	weight percent conversion
Δp	difference between p and $\hat{p}$
r_1, r_2	monomer reactivity ratios
$r_1{}^*$	true value of r_1
$\hat{r}_1$	final value (estimate) of r_1
$r_2{}'$, $r_2{}''$, $r_2{}^0$	approximations of r_2
$r_2{}^*$	true value of r_2
$\hat{r}_2$	final value (estimate) of $\hat{r}_2$
Δr_2	difference between r_2 and $\hat{r}_2$
x	ratio of $[M_1]_0$ and $[M_2]_0$
x_1	ratio of $[M_1]$ and $[M_1]_0$
x_2	ratio of $[M_2]$ and $[M_2]_0$
y	ratio of F_1 and F_2
A	value computed by eq 7a
A_0	value of A based on p^0 and $r_2{}^0$
B	value computed by eq 7b
B_0	value of B based on p^0 and $r_2{}^0$
C	value computed by eq 7c
C_0	value of C based on p^0 and $r_2{}^0$
D_0	parameter related to A_0, B_0, and C_0 (eq A-26)
F	independent variable of FR equation
F_1	instantaneous mole fraction of monomer 1 in the copolymer
$F_1{}^*$	true value of F_1
F_2	instantaneous mole fraction of monomer 2 in the copolymer
$F_\theta(2,n-2)$	value of θ percentage point of tabulated F distribution with 2 and $(n - 2)$ degrees of freedom
G	dependent variable of FR equation
M	value computed by eq A-31
M_1	molecular weight of monomer 1
M_2	molecular weight of monomer 2
$[M_1]$	instantaneous concentration of monomer 1
$[M_1]_0$	initial concentration of monomer 1
$[M_2]$	instantaneous concentration of monomer 2
$[M_2]_0$	initial concentration of monomer 2
N	value computed by eq A-32
Q	variable defined by eq 4a
R	variable defined by eq A-35
$\overline{\Delta R}$	accuracy index defined by eq 16
S	parameter defined by eq 5
$S_m{}^2$	estimate of the experimental error variance (eq A-27)
W	weight of the function f
W'	weight W based on p' and $r_2{}'$
X	variable defined by eq 4b

References and Notes

(1) Koenig, J. L. In *Chemical Microstructure of Polymer Chains*; Wiley: New York, 1980.

(2) Garcia-Rubio, L. H.; MacGregor, J. F.; Hamielec, A. E. *ACS Symp. Ser.* **1982**, *No. 197*, 87.

(3) McFarlane, R. C.; Reilly, P. M.; O'Driscoll, K. F. *J. Polym. Sci.* **1980**, *18*, 251.

(4) van der Meer, R.; Linssen, H. N.; German, A. L. *J. Polym. Sci., Polym. Chem. Ed.* **1978**, *16*, 2915.

(5) Kelen, T.; Tudos, F. *J. Macromol. Sci., Chem.* **1975**, *A9*(1), 1.

(6) Tidwell, P. W.; Mortimer, G. A. *J. Macromol. Sci., Rev. Macromol. Chem.* **1970**, *C4*(2), 281.

(7) Laurier, G. C.; O'Driscoll, K. F.; Reilly, P. M. *J. Polym. Sci., Polym. Symp.* **1985**, *72*, 17.

(8) O'Driscoll, K. F.; Kale, L. T.; Garcia-Rubio, L. H.; Reilly, P. M. *J. Polym. Sci., Polym. Chem. Ed.* **1984**, *22*, 2777.

(9) Alfrey, T., Jr.; Goldfinger, G. *J. Chem. Phys.* **1944**, *12*, 205.

(10) Mayo, F. R.; Lewis, F. M. *J. Am. Chem. Soc.* **1944**, *66*, 1594.

(11) Skeist, I. *J. Am. Chem. Soc.* **1946**, *68*, 1781.

(12) Meyer, V. E.; Lowry, G. G. *J. Polym. Sci., Part A* **1965**, *3*, 2843.

(13) Fineman, M.; Ross, S. D. *J. Polym. Sci.* **1950**, *5*, 269.

(14) Behnken, D. W. *J. Polym. Sci., Part A* **1964**, *2*, 645.

(15) Tidwell, P. W.; Mortimer, G. A. *J. Polym. Sci., Part A* **1965**, *3*, 369.

(16) Yamada, B.; Itahashi, M.; Otsu, T. *J. Polym. Sci.* **1978**, *16*, 1719.
(17) Patino-Leal, H.; Reilly, P. M.; O'Driscoll, K. F. *J. Polym. Sci., Part C* **1980**, *18*, 219.
(18) Reilly, P. M.; Patino-Leal, H. *Technometrics* **1981**, *23*, 221.
(19) Garcia-Rubio, L. H., Ph.D. Dissertation; McMaster University, 1981.
(20) Wentworth, W. E. *J. Chem. Educ.* **1965**, *42*, 96.
(21) The program was written in Fortran and is available on request from the authors.
(22) Sutton, T. L.; MacGregor, J. F. *Can. J. Chem. Eng.* **1977**, *55*, 602.
(23) Draper, N. R.; Smith, H. *Applied Regression Analysis*, 2nd ed.; Wiley: New York, 1981.

Computer Simulations of Radiation-Cured Networks

L. Y. Shy and B. E. Eichinger*

Department of Chemistry, BG-10, University of Washington, Seattle, Washington 98195.

Received June 17, 1986

ABSTRACT: Simultaneous cross-linking and chain scission reactions that are induced by ionizing radiation have been simulated with a computer. These studies were performed for both bulk- and solution-cured poly(dimethylsiloxane) (PDMS) systems. Variations of network structures and mechanical properties that depend on the degree of cross-linking are presented. It is shown that radiation-cured networks are barely connected and contain large amounts of defect structures. More than 90% of the defects are found to be dangling ends, and isolated ends are dominant in this population. The weight fraction of loops is quite small, but they deplete a large fraction of the cross-links. These results are in good agreement with experiment and with other calculations. Potential correlations between network structures and the Mooney–Rivlin coefficients $2C_1$ and $2C_2$ are also discussed.

1. Introduction

Networks that are cured through radiation-induced random cross-linking are of considerable commercial and laboratory interest. Numerous studies[1–8] have resulted in the characterization of the radicals that are formed, the yield of evolved gas, changes in viscosity, and the cross-linking densities of the networks. There is, however, much more to be understood. For instance, the extent and mechanism of backbone scission and rearrangement remain obscure. Moreover, we still do not know if network structures that have suffered radiation damage have altered dynamic mechanical properties.

Owing to the absence of analytical techniques for direct investigation of network structures, our understanding of them has been mainly from theoretical considerations. The first model calculation on randomly cross-linked networks was done by Tonelli and Helfand[9] for *cis*-1,4-polyisoprene (PIP). They calculated probability density functions to estimate the fraction of cross-links, as well as polymer, that are wasted in ends and loops. It was found that the weight fraction of elastically ineffective material is large and that the fraction of polymer contained in loops becomes significant for the case of solution curing. This result has provoked speculation that there might be some correlation between elastically ineffective material and the Mooney–Rivlin coefficient $2C_2$. More recently, Queslel and Mark[10] formulated a theory for the densities of active chains, active junctions, and the cycle rank for regular networks having only isolated ends. Their method is here extended to the case where chain scission is appreciable, which is especially the case for high-energy radiation.

Computer simulations prove to be powerful for network structure problems. Our previous work on end-linking systems shows that not only can the network structures[11,12] be well resolved by the use of simulation, but questions related to sol–gel transitions[13] and mechanical properties[11,14,15] can all be nicely addressed. Wherever there is sufficient knowledge of the reaction system and enough data for comparison, computer simulations can provide information with depth and accuracy that cannot be obtained in any other way.

We have modified our algorithms to enable us to simulate the simultaneous chain scission and cross-linking reactions that are induced by ionizing radiation. These studies have been performed for both bulk- and solution-cured PDMS systems, and the results will here be compared with experiments.[7,8] It will be demonstrated that computer model calculations can be used to great effect, even though there are very little available data to build upon.

2. Survey of Radiation Chemistry

Upon irradiation with high-energy radiation (electron beam or γ-ray), macromolecules will generally yield chain-end and side-chain macroradicals:

$$\sim\sim\sim\sim\sim\sim\sim\sim \xrightarrow{\text{irradiation}}$$

(1) main-chain scission $\sim\sim\sim\sim\cdot + \cdot\sim\sim\sim\sim$
(2) side-chain dissociation $\sim\sim\sim\sim\dot{\sim}\sim\sim\sim\sim + \cdot R_1$

Here $\cdot R_1$ is a fragment from the side chain of a macromolecule, which may be $\cdot CH_3$ or $\cdot H$ for PDMS. Solvent, if present, may also be dissociated. It should be noted that although we refer to these products as radicals, there is also evidence for ionic mechanisms from previous chemical studies.[2,4–6] Macroradicals can be deactivated by interaction with solvent molecules and fragment radicals, and new radicals can be generated by energy transfer and hydrogen abstraction. To form a cross-linkage, a side-chain macroradical recombines either with another to give a tetrafunctional cross-link or with a chain-end radical to yield a trifunctional junction. These two types of macroradicals are expected to have quite different reactivities, due to steric constraints and the cage effect. Cross-links with higher functionalities are also likely for some unsaturated polymers. This, however, is not believed to be the case[16] for PDMS.

The experimental data that are addressed by these simulations were reported[7,8] by Mark, Johnson, and Yu. PDMS with 6800 monomer units ($M_n = 0.5 \times 10^6$) was cross-linked with γ-radiation from a ^{60}Co source at room temperature. Various radiation doses were applied at